Synthesis, structure, and properties of $Ba_9Co_3Se_{15}$ with one-dimensional spin chains*

Lei Duan(段磊)[1,2], Xian-Cheng Wang(望贤成)[1,†], Jun Zhang(张俊)[1,2], Jian-Fa Zhao(赵建发)[1,2], Li-Peng Cao(曹立朋)[1,2], Wen-Min Li(李文敏)[1,2], Run-Ze Yu(于润泽)[1], Zheng Deng(邓正)[1], and Chang-Qing Jin(靳常青)[1,2,3,‡]

[1] *Institute of Physics, Chinese Academy of Sciences, Beijing* 100190, *China*
[2] *School of Physics, University of Chinese Academy of Sciences, Beijing* 100190, *China*
[3] *Materials Research Laboratory at Songshan Lake, Dongguan* 523808, *China*

(Received 26 November 2019; revised manuscript received 6 January 2020; accepted manuscript online 10 January 2020)

A new compound with one-dimensional spin chains, $Ba_9Co_3Se_{15}$, was synthesized under high pressure and high temperature conditions and systematically characterized via structural, transport and magnetic measurements. $Ba_9Co_3Se_{15}$ crystallizes in a hexagonal structure with the space group P-6c2 (No. 188) and lattice constants of $a = b = 9.6765$ Å and $c = 18.9562$ Å. The structure consists of trimeric face-sharing octahedral $CoSe_6$ chains, which are arranged in a triangular lattice in the ab-plane and separated by Ba atoms. The distance of the nearest neighbor of $CoSe_6$ chains is very large, given by the lattice constant $a = 9.6765$ Å. The Weiss temperature T_θ associated with the intra-chain coupling strength is about -346 K. However, no long-range magnetic order but a spin glass transition at ~ 3 K has been observed. Our results indicate that the spin glass behavior in $Ba_9Co_3Se_{15}$ mainly arises from the magnetic frustration due to the geometrically frustrated triangular lattice.

Keywords: one-dimensional chain, spin glass, high-pressure

PACS: 61.05.cp, 61.50.–f, 61.66.Fn, 61.82.Fk **DOI:** 10.1088/1674-1056/ab69ea

1. Introduction

Quasi-one-dimensional (1D) system exhibits many exotic physical phenomena due to the reduction of dimensions. It is well known that for an ideal 1D spin chain, the thermal and quantum fluctuations prevent the formation of a long-range order at finite temperature.[1] However, for a system with quasi 1D spin chains, the inter-chain spin interaction usually results in the long-range magnetic transition although it generally is very weak. It is especially interesting when these spin chains are arranged in a triangular lattice, which would induce geometric magnetic frustration and give rise to rich ground states. The prominent example is the composition ABX_3 (A is alkali metal, B is 3d transition metal, X is halogen atom), where the infinite face-sharing BX_6 octahedral chains are triangularly arranged in the ab-plane.[2] For these ABX_3 compounds, the intra-chain exchange interaction is typically two to three orders of magnitude larger than the inter-chain coupling, presenting strongly 1D magnetic properties. Complex spin arrangements in the ABX_3 compounds have been reported due to the frustrated antiferromagnetic interaction.[3–10] To partially relieve the frustration effect, the spins on the three sublattices usually form 120° angles with the nearest neighbors on the other sublattices for Heisenberg triangular antiferromagnets. While for Ising triangular antiferromagnets ($CsCoCl_3$[3,5] and $CsCoBr_3$[10]), the frustration effect becomes more acute and leads to either partial ordered state or fully ordered ferromagnetic state in the triangular plane.

Besides the triangular antiferromagnet of halogenides, the isostructural chalcogenide $BaVS_3$ with octahedral VS_6 chains has been extensively studied.[11–14] A metal–insulator transition at 69 K driven by Peierls instability was observed and in sequence an incommensurate antiferromagnetic transition occurred at ~ 31 K.[11] When the S atoms in $BaVS_3$ were replaced with Se, $BaVSe_3$ was reported to be a ferromagnetic metal.[15] Recently, in order to further enhance the distance of the nearest neighbor chains to enhance the 1D nature, $Ba_9V_3Se_{15}$ has been synthesized, which undergoes a ferrimagnetic transition at 2.5 K and presents 1D ferromagnetic chains properties, i.e., $T^{1/2}$ magnetic specific heat above the ordered temperature.[16]

Here, we report a new compound $Ba_9Co_3Se_{15}$, which is isostructural with $Ba_9V_3Se_{15}$, consisting of trimerized face-sharing octahedral $CoSe_6$ chains. Although the Weiss temperature associated with the intra-chain coupling strength is about -346 K, no long-range order but spin glass ground state is observed with the frozen temperature $T_f \sim 3$ K, which is speculated to be caused by the magnetic frustration due to the geometrically frustrated triangular lattice in $Ba_9Co_3Se_{15}$.

*Project supported by the National Key R&D Program of China and the National Natural Science Foundation of China (Grant Nos. 2018YFA0305700, 2017YFA0302900, 11974410, and 11534016).

†Corresponding author. E-mail: wangxiancheng@aphy.iphy.ac.cn
‡Corresponding author. E-mail:jin@iphy.ac.cn

2. Experimental methods

The synthesis of $Ba_9Co_3Se_{15}$ was carried out under high pressure and high temperature conditions using a DS 6×800 T cubic anvil high-pressure apparatus. The fine powders of Co (Alfa, 99.99% pure) and Se (Alfa, 99.999% pure), and lumps of Ba (Alfa, immersed in oil, $>99.2\%$ pure) were used as the starting materials. The precursor BaSe was prepared through the reaction of the Ba blocks and Se powder in an alumina crucible sealed in an evacuated quartz tube at 700 ℃ for 24 h. The mixture of BaSe, Co, and Se was homogenously mixed at the molar ratio of 3 : 1: 2, pressed into a pellet with a diameter of 6 mm, and then subjected to high-pressure synthesis under 5.5 GPa and 1000 ℃ for 40 min. The pressure was released after the temperature was quenched to room temperature, after which the black polycrystalline sample of $Ba_9Co_3Se_{15}$ was obtained.

The x-ray diffraction (XRD) was conducted on a Rigaku Ultima VI (3 kW) diffractometer using Cu K_α radiation generated at 40 kV and 40 mA. The Rietveld refinements on the diffraction patterns were performed using the GSAS software package.[17] The chemical composition of the $Ba_9Co_3Se_{15}$ sample was determined through energy dispersive x-ray spectroscopy (EDX). The electrical resistivity $\rho(T)$ and ac magnetic susceptibility measurements were carried out in a physical property measuring system (PPMS), and the dc magnetic susceptibility was measured by a superconducting quantum interference device (SQUID-VSM, Quantum Design).

3. Results and discussion

Polycrystalline sample of $Ba_9Co_3Se_{15}$ was synthesized under high-pressure and high-temperature conditions. The chemical composition of $Ba_9Co_3Se_{15}$ was determined by EDX as shown in Fig. 1(a). The inset shows the shining surface of the sample with the grain size about 40 μm. EDX measurement was performed at several different areas on the surfaces, and the average atomic ratio of Ba : Co : Se is about 3.02 : 0.95 : 5.01, which is very close to the stoichiometric ratio of $Ba_9Co_3Se_{15}$.

The powder XRD pattern measured at room temperature is shown in Fig. 1(b). All the peaks can be indexed by a hexagonal structure with the lattice parameters of $a=b=9.6765$ Å and $c=18.9562$ Å. The crystal structure of recently discovered compound $Ba_9V_3Se_{15}$ with a hexagonal structure and the space group P-6c2 (No. 188) was adopted as the initial model to refine the diffraction data of $Ba_9Co_3Se_{15}$. By using GSAS software packages, the refinements were conducted and smoothly converged to $\chi^2=3.16$, $R_p=3.24\%$, $R_{wp}=4.61\%$. The obtained crystallographic data and some selected interatomic distances are summarized in Table 1.

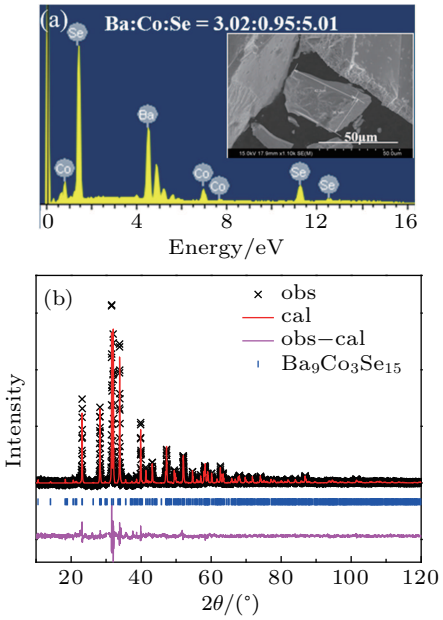

Fig. 1. (a) Energy dispersive x-ray spectrum collected on $Ba_9Co_3Se_{15}$ polycrystalline samples. (b) Powder XRD patterns of $Ba_9Co_3Se_{15}$ measured at 300 K and the refinement with the space group of P-6c2 (No. 188).

Table 1. Crystallographic data of $Ba_9Co_3Se_{15}$ and some selected interatomic distances in $Ba_9Co_3Se_{15}$.

Compound			$Ba_9Co_3Se_{15}$			
Space group: P-6c2 (No. 188), hexagonal						
$a=b=9.6765(2)$ Å, $c=18.9562(6)$ Å						
$V=1546.16(5)$ Å^3, $Z=2$						
$\chi^2=3.16$, $R_p=3.24\%$, $R_{wp}=4.61\%$						
Atom	Label	Wyck	x/a	y/b	z/c	SOF
Ba	Ba1	12l	0.00688	0.36705	0.08638	1
Ba	Ba2	6k	0.38548	0.38687	1/4	1
Co	Co1	2a	0	0	0	1
Co	Co2	4g	0	0	0.16095	1
Se	Se1	12l	0.24526	0.25423	0.08187	1
Se	Se2	6k	−0.01531	0.20961	1/4	1
Se	Se3	2c	1/3	2/3	0	1
Se	Se4	4h	1/3	2/3	0.18645	1
Se	Se5	4i	2/3	1/3	0.16786	1
Se	Se6	4i	2/3	1/3	0.04253	0.5
Selected interatomic distances in $Ba_9Co_3Se_{15}$/Å						
Co1–Co2		3.051		Co2–Co2		3.376
Se3–Se4		3.534		Se4–Se4		2.409
Se5–Se6		2.376		Se5–Se5		3.114

Figure 2(a) presents the sketch of the crystal structure of $Ba_9Co_3Se_{15}$. The structure consists of infinite face-sharing octahedral $CoSe_6$ chains along c axis, and these chains are triangularly arranged in the ab-plane and separated by Ba and Se atoms, demonstrating the 1D structural character. The $CoSe_6$ chains are trimerized, leading to two sites of Co(1) and Co(2), as shown in Fig. 2(b). The distances between adjacent Co atoms in chains $d_{in-chain}$ are 3.051 Å and 3.376 Å, respectively, while the distance between nearest neighbor Co atoms in the ab-plane $d_{in-plane}$ is given by the lattice constant $a=9.6765$ Å, significantly larger than $d_{in-chain}$. We can compare the values of $d_{in-chain}$ and $d_{in-plane}$ with those

of $CsCoBr_3$, which has a similar chain structure with the infinite face-sharing octahedral $CoBr_6$ chains separated by Cs^+ ions. For $CsCoBr_3$, the in-chain distance $d_{\text{in-chain}}$ is 3.162 Å, which is very close to that in $Ba_9Co_3Se_{15}$, while the in-plane distance $d_{\text{in-plane}} = 7.529$ Å is much smaller than the value in $Ba_9Co_3Se_{15}$.[18] It was reported that the intra-chain coupling strength (~ 6.7 meV) is more than fifteen times larger than the inter-chain exchange interaction (~ 0.4 meV) in $CsCoBr_3$.[6] Thus, compared with $CsCoBr_3$, the significantly larger $d_{\text{in-plane}}$ in $Ba_9Co_3Se_{15}$ suggests an even weaker inter-chain coupling strength and makes $Ba_9Co_3Se_{15}$ further approach to the nature of 1D spin chain in the view of crystal structure. Besides the $CoSe_6$ chains, there exist Se-chains at the center of the triangular lattice, where the Se atoms occupy the Se(3)–Se(4) and Se(5)–Se(6) sites, respectively, as shown in Fig. 2(c). The distances of the adjacent Se atoms in the Se-chains range from 2.376 Å to 3.534 Å. The small distances of 2.376 Å and 2.409 Å are very close to the Se–Se bond length, which implies the formation of Se_2^{2-} dimer in the Se-chains. The similar Se_2^{2-} (Te_2^{2-}) dimer has also been reported in $Ba_9V_3Se_{15}$[16] and $Ba_9Sn_3Se_{15}$ ($Ba_9Sn_3Te_{15}$).[19]

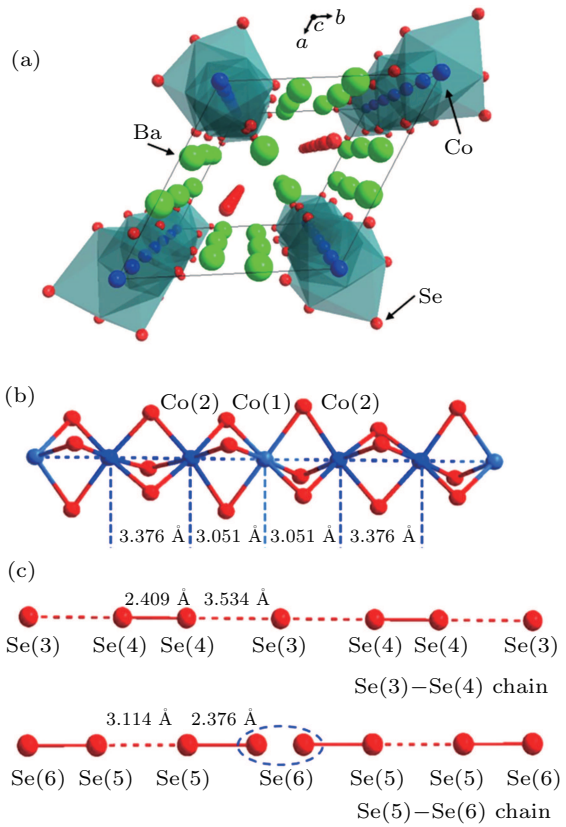

Fig. 2. The crystal structure of $Ba_9Co_3Se_{15}$. (a) Top view with the projection along c axis for $Ba_9Co_3Se_{15}$. (b) and (c) The sketch of octahedral $CoSe_6$ chains and Se chains in $Ba_9Co_3Se_{15}$.

The temperature dependence of resistivity in $Ba_9Co_3Se_{15}$ is shown in Fig. 3(a). The resistivity increases with decreasing temperature, demonstrating a semiconducting behavior. The inset of Fig. 3(a) is the plot of $\ln\rho$ versus $1/T$. The curve of $\ln\rho(1/T)$ is a straight line in the whole measured temperature range, which indicates that the semiconducting behavior can be described based on the Arrhenius law for thermally activated conduction. By using the formula $R \propto \exp(\Delta_g/2k_BT)$, where Δ_g is the semiconducting band gap and k_B is the Boltzmann's constant, the resistivity curve is well fitted and Δ_g is calculated to be 0.748 eV, which is larger than those of $Ba_9Sn_3Se_{15}$ (~ 0.5 eV)[19] and $Ba_9V_3Se_{15}$ (~ 0.2 eV).[16]

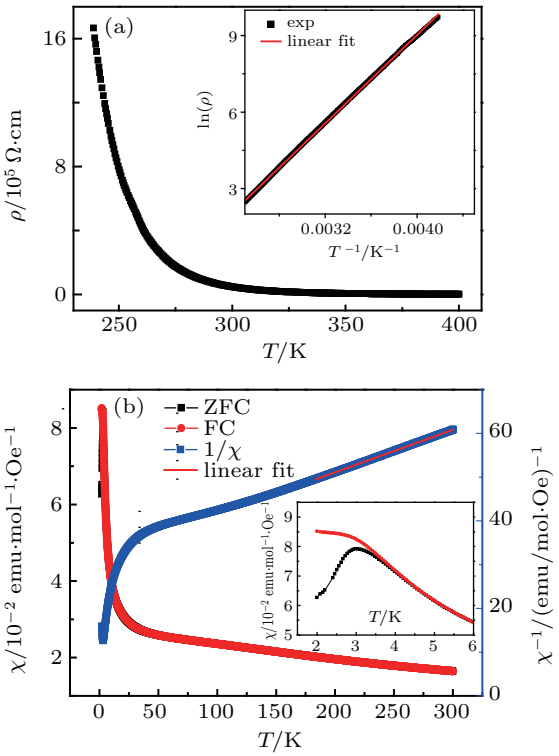

Fig. 3. (a) The temperature dependence of resistivity, the inset shows $\ln\rho$ versus $1/T$. (b) The magnetic susceptibility χ as a function of temperature under ZFC and FC conditions and the reverse susceptibility versus temperature. The red line is the fit of Curie–Weiss law between 200 K and 300 K. The inset shows the low temperature parts.

In order to study the magnetic properties, the dc magnetic susceptibility as a function of temperature was measured under the magnetic field of 1000 Oe in both zero-field-cooled (ZFC) and field-cooled (FC) modes, as shown in Fig. 3(b). The ZFC and FC curves are overlapped and begin to bifurcate at about 5 K, which demonstrates a λ-shape and suggests a spin-glass ground state with the frozen temperature about 3 K, as shown in the inset of Fig. 3(b). The inverse susceptibility versus temperature is also plotted in Fig. 3(b). In the high temperature region, the susceptibility shows a Curie–Weiss paramagnetic behavior. After fitting the susceptibility in this paramagnetic region by using the Curie–Weiss law $\chi = C/(T - T_\theta)$, the Weiss temperature and effective moment can be obtained to be $T_\theta = -324$ K and $\mu_{\text{eff}} = 5.2\ \mu_B$ per Co ion, respectively. The negative sign of T_θ indicates that the predominant interaction is antiferromagnetic. The μ_{eff} value is typical for Co^{2+} (d^7, $S = 3/2$), ranging from 4.3 μ_B to 5.2 μ_B.[20–23] The g factor calculated from the Curie constants ($\mu_{\text{eff}}^2 = g^2S(S+1)$) is

2.70, and the large g factor for the Co^{2+} systems is considered to arise from the strong spin–orbital coupling and the large anisotropy.[20,21]

To verify the spin-glass feature, we carried out the ac magnetic susceptibility measurement. The temperature dependence of the real part of the ac susceptibility χ' is shown in Fig. 4(a). Four frequencies, ranging from 133 Hz to 6373 Hz, are used to study the dynamic response of the macroscopic susceptibility. All the ac susceptibility χ' curves display a peak at the frozen temperature T_f, with the shape similar to that of the ZFC curve of the dc susceptibility. The maximum value of χ' decreases as the frequency increases. In addition, the frozen temperature T_f is sensitive to the frequency, which increases from 3.5 K to 4 K when the frequency increases from 133 Hz to 6373 Hz, confirming the spin-glass ground state of $Ba_9Co_3Se_{15}$. To characterize the spin glass, the response of susceptibility on the frequency can be quantified by the coefficient $K = \Delta T_f/(T_f \Delta \log f)$, as shown in Fig. 4(b). Here, for $Ba_9Co_3Se_{15}$, $K = 1.6 \times 10^{-2}$ lies in the range of 5×10^{-3}–8×10^{-2} for a typical spin glass system.[24]

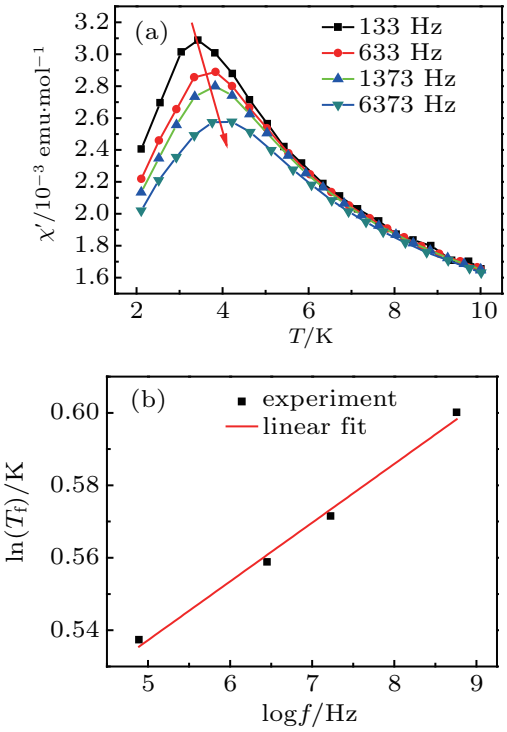

Fig. 4. (a) The temperature dependence real part of ac magnetic susceptibility (χ') at different frequencies. (b) $\ln T_f$ vs. $\log f$ plot for $Ba_9Co_3Se_{15}$.

$Ba_9Co_3Se_{15}$ possesses a strong quasi 1D spin chain characteristic and a triangular arrangement tending to induce geometric magnetic frustration. The octahedral $CoSe_6$ chains are arranged in a triangular lattice in the *ab*-plane with a significantly large distance, demonstrating a 1D chain structure. Generally, there are two energy scales for a quasi 1D spin chain system, one is the intra-chain spin coupling strength J_{intra} associated with the Weiss temperature, and the other is the inter-chain spin exchange interaction strength J_{inter}, which is usually much weaker than the intra-chain coupling and related with the temperature of long-range order formation. Using the Weiss temperature T_θ obtained from the magnetic susceptibility measurement, we can estimate the value of J_{intra} to be about 69 K via the equation $kT_\theta = \frac{2z}{3}S(S+1)J$, where $z = 2$ is the number of neighbor magnetic ions in the spin chain and $S = 3/2$ is the spin moment. The frozen temperature T_f in $Ba_9Co_3Se_{15}$ with a spin-glass ground state is comparable with the ferromagnetic transition temperature of 2.5 K observed in the isostructural $Ba_9V_3Se_{15}$, which hints that the inter-chain exchange interaction J_{inter} is very weak. Magnetic frustration usually happens in the system with the antiferromagnetic coupled spins on the triangular lattice, kagomé lattice, and pyrochlore lattice.[25] To partially release the magnetic frustration of a triangular lattice, the spins on the triangular lattice can form 120° angles with nearest neighbors for Heisenberg triangular antiferromagnets, and the spins can be partially ordered or fully ordered with up–up–down arrangement for Ising triangular antiferromagnets.[2] While for the other triangular-lattice compounds of candidate of spin-liquid state, such as $YbZnGaO_4$[26] and κ-(BEDT-TTF)$_2$Cu$_2$(CN)$_3$,[27] the spin-glass ground state was recently confirmed for the former and considered to be driven by the magnetic frustration and disorder, for the latter, no long-range order has been observed down to 75 mK and the magnetic frustration was suggested to lead to a spin-liquid state. Here, the observed spin glass behavior in $Ba_9Co_3Se_{15}$ is speculated to mainly arise from the geometric magnetic frustration.

4. Conclusion and perspectives

The new quasi one-dimension spin chain compound $Ba_9Co_3Se_{15}$ has been synthesized under high pressure and high temperature conditions. It crystallizes into a hexagonal structure with the space group of *P*-6*c*2 (No. 188). The infinite face-sharing octahedral $CoSe_6$ chains are arranged in a triangular lattice and separated by a large distance. The compound displays a semiconducting behavior with a band gap ~ 0.748 eV and a spin-glass ground state with the freezing temperature $T_f = 3$ K. The Weiss temperature is deduced to be -346 K, indicating that the predominant intra-chain exchange interaction is antiferromagnetic. It is speculated that the spin glass behavior in $Ba_9Co_3Se_{15}$ mainly arises from the magnetic frustration due to the geometrically frustrated triangular lattice.

References

[1] Mermin N D and Wagner H 1966 *Phys. Rev. Lett.* **17** 1133
[2] Collins M F and Petrenko O A 1997 *Can. J. Phys.* **75** 605

[3] Boucher J P, Regnault L P, Rossat-Mignod J, Henry Y, Bouillot J and Stirling W G 1985 *Phys. Rev. B* **31** 3015

[4] Caciuffo R, Paolasini L, Sollier A, Ghigna P, Pavarini E, van den Brink J and Altarelli M 2002 *Phys. Rev. B* **65** 174425

[5] Goff J P, Tennant D A and Nagler S E 1995 *Phys. Rev. B* **52** 15992

[6] Mao M, Gaulin B D, Rogge R B and Tun Z 2002 *Phys. Rev. B* **66** 184432

[7] Morishita K, Kato T, Iio K, Mitsui T, Nasui M, Tojo T and Atake T 2000 *Ferroelectrics* **238** 105

[8] Nishiwaki Y, Tokunaga M, Nakamura T, Todoroki N and Kato T 2010 *J. Phys. Soc. Jpn.* **79** 084707

[9] Tennant D A, Perring T G, Cowley R A and Nagler S E 1993 *Phys. Rev. Lett.* **70** 4003

[10] Yelon W B, Cox D E and Eibschütz M 1975 *Phys. Rev. B* **12** 5007

[11] Fagot S, Foury-Leylekian P, Ravy S, Pouget J P and Berger H 2003 *Phys. Rev. Lett.* **90** 196401

[12] Gardner R A, Vlasse M and Wold A 1969 *Acta Cryst.* **25** 781

[13] Imai H, Wada H and Shiga M 1996 *J. Phys. Soc. Jpn.* **65** 3460

[14] Nakamura H, Yamasaki T, Giri S, Imai H, Shiga M, Kojima K, Nishi M, Kakurai K and Metoki N 2000 *J. Phys. Soc. Jpn.* **69** 2763

[15] Ana Akrap, Vladan Stevanović Mirta Herak, Marko Miljak, Barišić N, Berger H and Forró L 2008 *Phys. Rev. B* **78** 235111

[16] Zhang J, Liu M, Wang X, Zhao K, Duan L, Li W, Zhao J, Cao L, Dai G, Deng Z, Feng S, Zhang S, Liu Q, Yang Y F and Jin C 2018 *J. Phys.: Condens. Matter* **30** 214001

[17] Larson A C and Dreele R B V 1994 *Los Alamos Natl. Lab. Rep.* **86** 748

[18] Nagler S E, Buyers W J L, Armstrong R L and Briat B 1983 *Phys. Rev. B* **27** 1784

[19] Zhang J, Su R, Wang X, Li W, Zhao J, Deng Z, Zhang S, Feng S, Liu Q, Zhao H, Guan P and Jin C 2017 *Inorg. Chem. Front.* **4** 1337

[20] Hellwege K -H and Hellwege A M 1966 *Landolt-Börnstein New Series*, Vol. II/2

[21] Yang T, Zhang Y, Yang S H, Li G B, Xiong M, Liao F H and Lin J H 2008 *Inorg. Chem.* **47** 2562

[22] Mandrus D, Sarrao J L, Chakoumakos B C, FernandezBaca J A, Nagler S E and Sales B C 1997 *J. Appl. Phys.* **81** 4620

[23] Barnes A D J, Baikie T, Hardy V, Lepetit M B, Maignan A, Young N A and Francesconi M G 2006 *J. Mate. Chem.* **16** 3489

[24] Binder K and Young A P 1986 *Rev. Mod. Phys.* **58** 801

[25] Balents L 2010 *Nature* **464** 199

[26] Ma Z, Wang J H, Dong Z Y, Zhang J, Li S C, Zheng S H, Yu Y J, Wang W, Che L Q, Ran K J, Bao S, Cai Z W, Cermak P, Schneidewind A, Yano S, Gardner J S, Lu X, Yu S L, Liu J M, Li S Y, Li J X and Wen J S 2018 *Phys. Rev. Lett.* **120** 087201

[27] Yamashita S, Nakazawa Y, Oguni M, Oshima Y, Nojiri H, Shimizu Y, Miyagawa K and Kanoda K 2008 *Nat. Phys.* **4** 459